Acta Cryst. (1989). A**45**, 416-422

The Resolution Function of an X-ray Triple-Crystal Diffractometer: Comparison of Experiment and Theory

BY C. A. LUCAS, E. GARTSTEIN AND R. A. COWLEY

Department of Physics, University of Edinburgh, Mayfield Road, Edinburgh EH9 3JZ, Scotland

(*Received* 28 *June* 1988; *accepted* 16 *January* 1989)

Abstract

The resolution function of an X-ray triple-crystal diffractometer on a rotating-anode source has been studied both experimentally and theoretically. Three different experimental configurations were used, with perfect germanium, distorted germanium and pyrolytic graphite as monochromator and analyser, leading to changes in the resolution of two orders of magnitude. The results are compared with a Gaussian description of the resolution function and it is found that this describes the width of the central part with an accuracy of better than 25%. The wings of the resolution in the high-resolution mode show the effect of the non-Gaussian resolution elements but these are reproduced by a full numerical convolution theory of the resolution function.

I. Introduction

With the availability of intense X-ray sources, such as high-brilliance rotating-anode generators and synchrotron radiation sources, the triple-crystal X-ray diffractometer has found increasing use in high-resolution diffraction experiments. The ability to probe the reciprocal space of a sample crystal with a momentum resolution as small as 10^{-4} Å^{-1} has led to new results in the study of phase transitions (*e.g.* Ryan, Nelmes, Cowley & Gibaud, 1986) and of surfaces and interfaces (*e.g.* Andrews & Cowley, 1985; Robinson, 1986; Cowley & Ryan, 1987). However, even when using perfect crystals as monochromator and analyser, a thorough understanding of the instrumental resolution is required in order to measure quantitatively the nature of the scattered intensity in an experiment. In addition, a detailed knowledge of the resolution function in wave-vector space can enable the measurement of relatively weak diffuse scattering from critical fluctuations or surfaces, without interference from the strong scattering arising from the Bragg reflection (Andrews & Cowley, 1986).

Although the resolution function of a neutron three-axis spectrometer has been dealt with, both theoretically and experimentally, by several authors (Cooper & Nathans, 1967; Stedman, 1968; Bjerrum-Møller & Neilsen, 1970; Chesser & Axe, 1973), the corresponding calculation for an X-ray diffractometer has received comparatively little attention. The use of nearly perfect crystals for monochromator and analyser in the X-ray case means that their scattering must be described by dynamical diffraction theory (Zachariasen, 1945; Batterman & Cole, 1964). Reflection from a perfect crystal is then governed by the characteristic long-tailed asymmetric form of the Darwin profile, and not by the Gaussian form, assumed for the case of mosaic crystals, and used in the neutron scattering calculations. Unlike the Gaussian approximation, which may be solved largely analytically, convolution of these non-Gaussian profiles requires a complex numerical integration. Pynn, Fujii & Shirane (1983) have applied the formalism of Bjerrum-Møller & Neilsen (1970) to the case of the perfect-crystal X-ray diffractometer, and calculated the central part of the resolution function. They compared their calculations with experimental measurements of the peak shapes of the Bragg reflections from perfect germanium and silicon crystals and found good agreement. Recently Cowley (1987), following a suggestion by Pynn *et al.* (1983), approximated the results of the dynamical theory by a Gaussian, enabling the central part of the resolution function to be obtained analytically in terms of relatively simple expressions. It was hoped that, after convolution with other resolution elements, the calculations would be sufficiently accurate to allow a straightforward analysis of experimental results, and an easier planning of new experiments.

In this paper we report on further studies of the resolution function of a triple-crystal X-ray diffractometer with a rotating-anode source. Measurements of the resolution function of the diffractometer have been performed with three different sets of monochromator and analyser crystals; perfect germanium, distorted germanium and pyrolytic graphite. Measurements for a variety of different wave-vector transfers are described in § II, and these are compared with the widths calculated using the Gaussian approximation in § III. The tails of the resolution are far from Gaussian in form when perfect crystals are used for monochromator and analyser. This is because their scattering is described by the Darwin curve which has $1/\theta^2$ wings, rather than the more rapidly decreasing Gaussian wings assumed in the

0108-7673/89/060416-07$03.00

Gaussian theory. An understanding of these tails is essential if measurements are to be performed close to the Bragg reflections. In § II we present a qualitative description of the origin of these tails or streaks (Ryan, 1986). A quantitative description necessarily requires a numerical convolution over the different resolution elements. A computer program for doing such convolutions has recently been written (Gartstein, 1989) to calculate not only the central part of the resolution function, but also the wings down to the 10^{-3} level. In § III we compare the results of these calculations with the measurements and find very satisfactory agreement between experiment and theory. The results are discussed in a final section.

II. Experiments and results

1. *The experiments*

The experiments were performed at Edinburgh University using a triple-axis X-ray diffractometer based on a Huber 430/440 goniometer, and utilizing a GEC Avionics GX21 rotating-anode X-ray generator with a copper target. Cu $K\alpha_1$ X-rays (λ = 1·54051 Å, $\Delta\lambda$ = 0·00058 Å) were used, and the focal spot of the rotating-anode tube was a vertical line of height 3 mm and width 0·3 mm, viewed at a take-off angle of 6°. Fig. 1 shows a schematic picture of a triple-crystal X-ray diffractometer in the (+, −, +) configuration. This arrangement, in which $\theta_M = \theta_A \neq \theta_S$, was used throughout the experiments. A variable-width slit, immediately in front of the monochromator crystal, was used to limit the angular range of the X-ray beam incident on the monochromator and hence, for the germanium crystals, to eliminate the $K\alpha_2$ line. The monochromator was at a distance of 200 mm from the source. An additional slit, placed between the monochromator and sample crystals, limited the vertical divergence of the X-rays and ensured that the incident beam was fully intercepted by the sample. No other collimators were present between the monochromator crystal and the detector. The detector was a proportional counter with about 1·5 keV FWHM energy resolution at 8 keV.

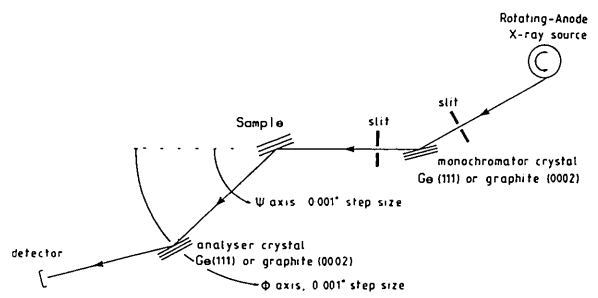

Fig. 1. Schematic diagram of a triple-crystal X-ray diffractometer.

Three different sets of crystals were used for the monochromator and analyser:

(1) *High resolution.* The 111 reflections of perfect germanium crystals were used for both monochromator and analyser. These reflections have a Darwin width of $4{\cdot}3 \times 10^{-3}$ °.

(2) *Intermediate resolution.* The 111 reflections from poor-quality germanium crystals were used as monochromator and analyser. These crystals had a measured mosaic spread (FWHM) of about 0·021°.

(3) *Low resolution.* The (0002) planes of pyrolytic graphite (Union Carbide UCAR grade ZYA) were used as monochromator and analyser. These crystals have a mosaic structure with an approximately Gaussian distribution of orientations and a mosaic spread of 0·4 (1)° (FWHM).

These three arrangements then provide for changes in the resolution of the diffractometer by two orders of magnitude.

Unfortunately the resolution function of the diffractometer cannot be measured directly, especially in its high-resolution mode, because the scattering from the sample is not a delta function in reciprocal space. Clearly the sample must be a material which has a perfect crystal structure, with a fairly large number of reciprocal-lattice points to enable the theory to be tested over a range of wave-vector transfers. We chose to use single crystals of InP or GaAs, grown in wafer form for use as substrates for the MBE growth of semiconductor heterostructures. The wafer had the [100] axis perpendicular

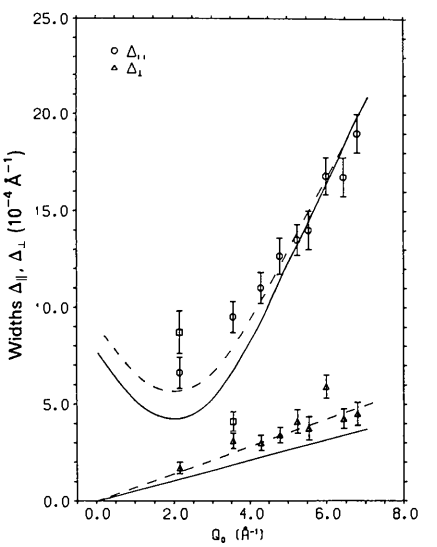

Fig. 2. The widths of the resolution function for the high-resolution mode with perfect germanium monochromator and analyser. The experimental results have been corrected for the Darwin width of the InP sample (circles). The correction is smaller than the error bars except for two low-Q points where the uncorrected data are shown by squares. The solid line is the calculated width using the theoretical Darwin width of Ge (111) planes and the dotted line is calculated with the Darwin width increased by 33%.

to the surface plane and was etched to remove any surface damage. The sample was oriented in an extended face geometry on the diffractometer, with either a [001] or [01$\bar{1}$] axis vertical and perpendicular to the scattering plane. Clearly the Darwin width of the InP or GaAs crystal has an effect on the observed scattering, especially in the high-resolution configuration. In this case in comparing experiment and theory it is necessary to incorporate the effect of the Darwin widths; this is described in § III.

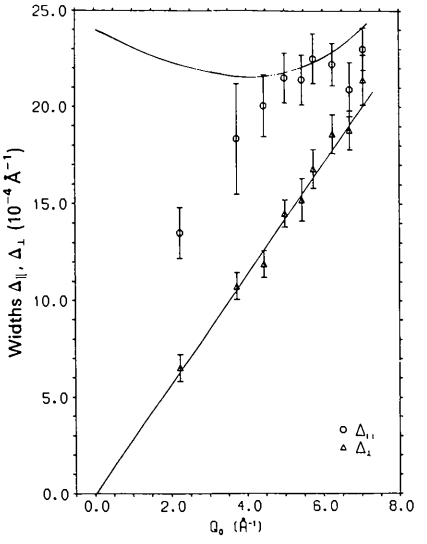

Fig. 3. The widths of the resolution function with the distorted Ge monochromator and analyser. The solid lines are the Gaussian theory with each Ge crystal having a mosaic width of 0·023°.

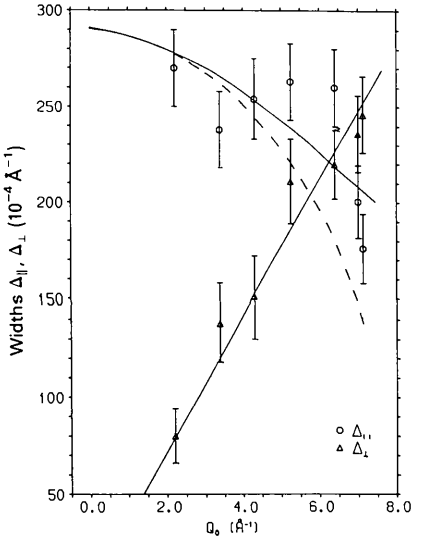

Fig. 4. The width of the resolution function with the pyrolytic-graphite monochromator and analyser. The dotted curve is the Gaussian theory with $\Delta\lambda/\lambda = 3{\cdot}5 \times 10^{-4}$ and mosaic 0·29°, while the solid curve has $\Delta\lambda/\lambda = 2{\cdot}5 \times 10^{-3}$.

For each experimental arrangement, the resolution function was measured in the transverse ($\delta Q_{\perp}$) and longitudinal ($\delta Q_{\parallel}$) directions by rocking the sample (a ψ scan in the notation of Fig. 1) or by scanning the sample and analyser arm in a ratio of 1:2 (ψ-φ = 2ψ scan). The ψ and φ axes had an angular precision of better than 0·001°. These measurements were performed for the InP 200, 400 and 600 symmetric reflections and for the 311, 422, 511 and 622 asymmetric reflections. The crystal was then rotated by 45° in the surface plane, enabling additional measurement at the 420, 440 and 620 Bragg reflections. For all the asymmetric reflections both shallow and deep entry angles of incidence were used, to study, for example, both the 311 and 3$\bar{1}\bar{1}$ reflections. The results of these experiments are shown in Figs. 2-4.

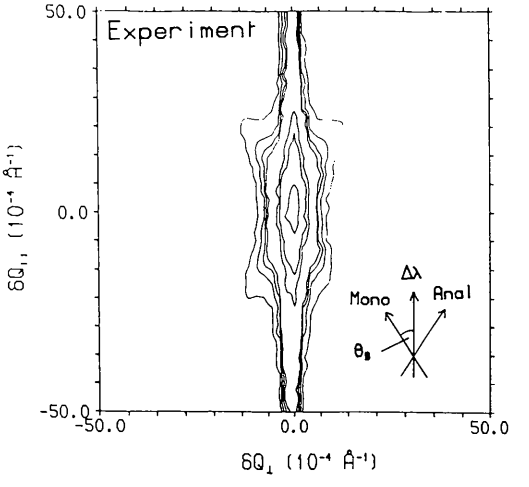

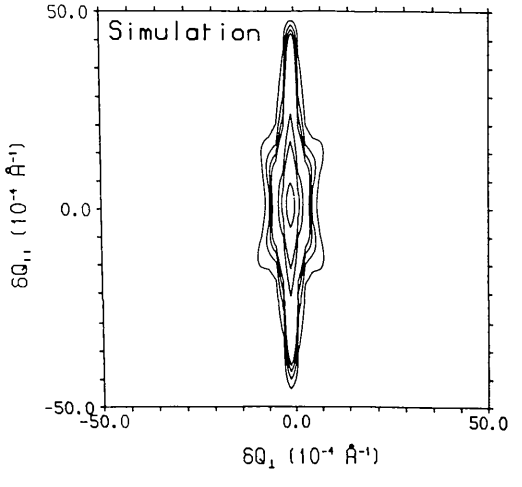

Fig. 5. A contour map of the scattered intensity in the high-resolution configuration around the InP 400 reflection as measured and as calculated by the convolution theory. The figure shows the directions of monochromator, analyser, and $\Delta\lambda$ streaks. The contour levels are 0·5, 0·1, 0·05, 0·01, 0·0075, 0·005 and 0·0025 of the peak intensity. The Bragg angle for this reflection, θ_B, is ~31·6°.

In addition to the measurements of the half-widths, a detailed study was made of the intensity distribution of the scattered X-rays around several of the Bragg reflections in the high resolution mode. The results are presented as contour maps with contours down to the 0·25% level in Figs. 5–7.

2. *Qualitative description of the resolution*

The high-resolution measurements shown in Figs. 5–7 are initially unexpected, in that the shape of the contours varies with their intensity level. The contours down to the 5% level are within error simple ellipses with the principal axes oriented parallel and perpendicular to the wave-vector transfer. This is as expected on the basis of the Gaussian theory of the resolution function (Cowley, 1987). The lower contours have a much more complex shape (Figs. 5–7), and these shapes cannot be explained by the Gaussian theory. These effects arise because the resolution-determining elements, the line width of the source, and the reflectivities of the perfect monochromator and analyser crystals, are not described by Gaussians but have larger wings dependent upon the square of the deviation from the nominal ray. As a result of this there are streaks corresponding to rays which pass through the central part of all except one of the resolution elements. Following the work of Ryan (1986) we now consider the location of these streaks in reciprocal space as an effect of each of the resolution elements in turn.

(*a*) *The monochromator.* The Darwin curve describing the reflectivity of the monochromator has $1/\delta\theta_M^2$ tails and these give rise to deviations in the direction of the incident beam. As illustrated in Fig. 8, if the angle of scattering at the sample is φ these then give rise to streaks at an angle $\varphi/2$ to the wave-vector transfer. Since the $1/\delta\theta^2$ tails arise from the surface scattering (Andrews & Cowley, 1985; Robinson, 1986) their effect can be reduced by using a monochromator with a rough surface, but the crystal structure must then remain perfect if the resolution is not to be degraded. If the monochromator is a mosaic

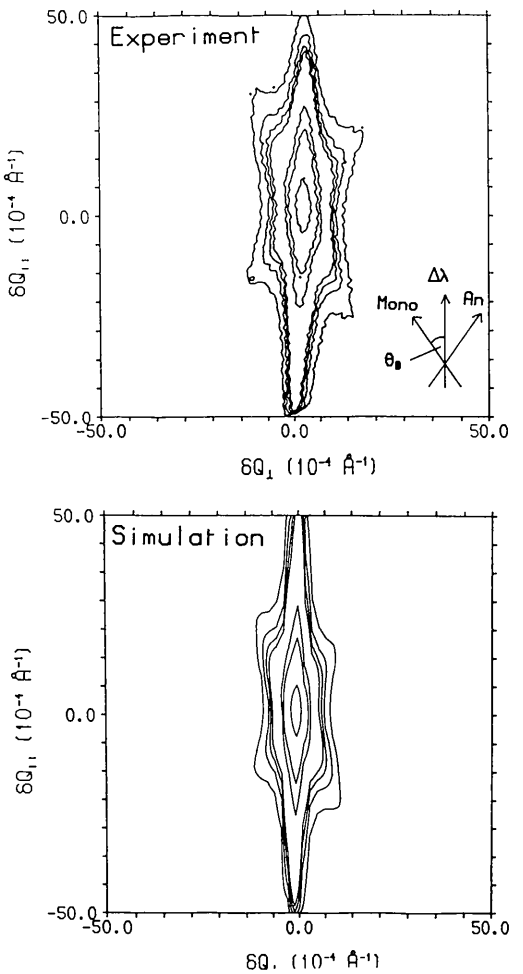

Fig. 6. The InP 420 reflection in the same representation as Fig. 5.

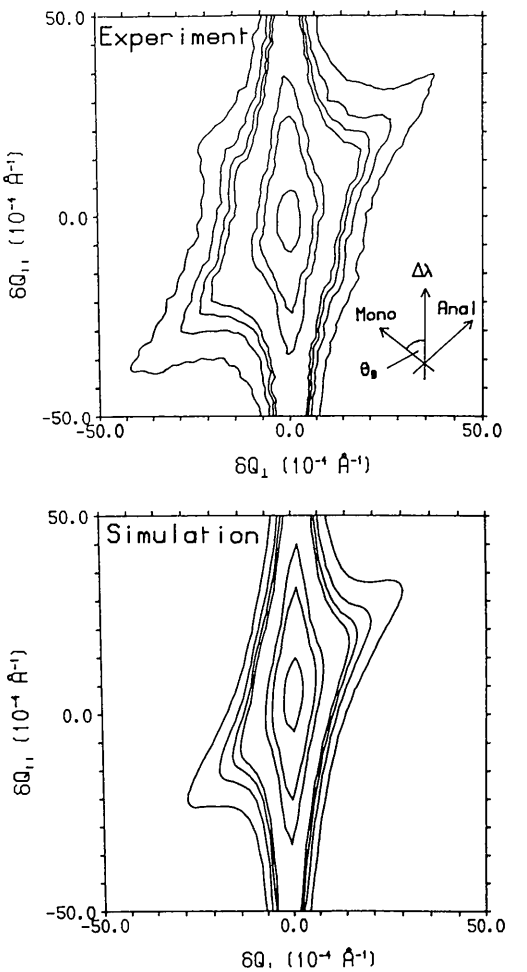

Fig. 7. The InP 4$\bar{4}$0 reflection in the same representation as Fig. 5.

crystal with different mosaic domains this may produce a similar streak with a form which reflects the mosaic structure.

(*b*) *The analyser.* The effect of the Darwin curve of the analyser is to allow deviations in the direction of the scattered beam, and so produces a streak perpendicular to that direction. As shown in Fig. 8, this is at an angle of $-\varphi/2$ to the wave-vector transfer. Experimentally it is usually found that this streak is more intense than that arising from the monochromator. Both of these streaks are clearly visible in Figs. 5-7.

(*c*) *The wavelength spread.* The characteristic line in the X-ray spectrum has a Lorentzian form, with $(1/\Delta\lambda)^2$ tails. Furthermore it is superimposed on the continuous spectrum which has $\sim 10^{-3}$ of the intensity of the characteristic line. For measurements at low levels of intensity it is then essential to understand the effects of the spread in incident wavelength. Experimentally the spread in wavelengths is reduced by a slit in front of the monochromator and the detailed shape of the effect of the wavelength spread depends critically on the positioning of this slit.

The effect of different wavelengths from a very small spot on the rotating anode is to give, after reflection on the monochromator, a beam whose direction depends on the wavelength or wave vector as shown in Fig. 8. For a triple-crystal spectrometer in the focusing configuration of Fig. 1, the change in the wave vector δk results in a change in the wave-vector transfer

$$\delta Q_{\parallel} = \delta k(2\tan\varphi/2 - \tan\theta_M - \tan\theta_A)\cos\varphi/2$$

$$\delta Q_{\perp} = \delta k(\tan\theta_M - \tan\theta_A)\sin\varphi/2.$$

In the usual symmetric case with $\theta_M = \theta_A$, this shows that the spread in wavelength is along the wave-vector transfer. As is well known, focusing occurs if the scattering angle $\varphi = 2\theta_M = 2\theta_A$.

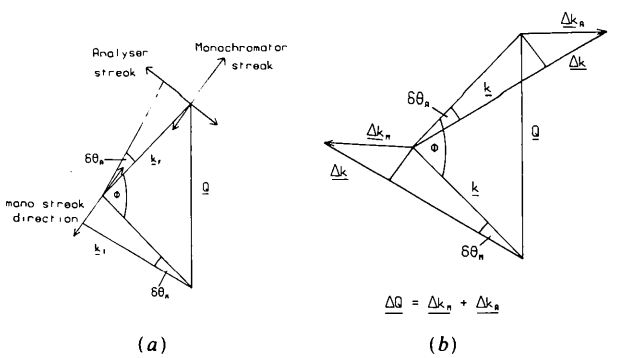

Fig. 8. The origin of the streaks in the wings of the resolution function. (*a*) The direction of the monochromator and analyser streaks. (*b*) The effect of a wavelength spread.

(*d*) *The specimen.* An ideal extended-face sample also has its reflectivity given by the Darwin curve, with $(1/\delta q)^2$ tails resulting from the surface scattering. Consequently the sample Bragg reflection is broadened in reciprocal space perpendicular to the extended face of the crystal in real space. For symmetric reflections, for which the wave-vector transfer is perpendicular to the sample surface, it is then impossible to distinguish between the $\Delta\lambda$ and specimen streaks unless the reflection is one with no wavelength dispersion. However, for asymmetric reflections the specimen and $\Delta\lambda$ streaks are in different directions.

In Figs. 5-7 the directions of the different streaks are clearly seen, and support the predictions of the simple theory given above. If the contour maps are extended to lower levels then these streaks become even more prominent.

III. Comparison with theory

1. *Gaussian theory*

The Gaussian theory of the resolution function is derived by assuming that all the resolution elements can be described by Gaussian response functions (Cowley, 1987). The theory then predicts that the resolution function is an ellipsoid in reciprocal space, with its principal axes parallel and perpendicular to the wave-vector transfer. Furthermore the theory gives explicit and relatively simple expressions for the widths of the resolution function.

In Fig. 2 we show the longitudinal and transverse widths of the resolution function as a function of wave-vector transfer. These were calculated using the theoretical Darwin width for the monochromator and analyser of $4{\cdot}3\times10^{-3}$ °. The experimental results were measured as described in § II, and corrected for the Darwin width of the InP sample crystal. The correction was calculated by using the Gaussian formalism and convoluting the calculated resolution function with a Gaussian representing the sample Darwin width. Except for the two reflections at the smallest wave-vector transfers, 200 and 311, the resulting corrections were smaller than the error bars. For these two points both the uncorrected widths and corrected widths are shown in Fig. 2. The experimental results are clearly in reasonable agreement with the theory, especially in view of the fact that there are no adjustable parameters in the theoretical calculations. Nevertheless the calculated transverse widths are approximately 75% of the measured ones and the minimum in the longitudinal widths at 2 Å^{-1} is also too small. Both of these features are largely dependent on the germanium Darwin widths of the monochromator and analyser, whereas the longitudinal widths for wave vectors $Q = 5$-7 Å^{-1}, which are largely dependent on the wavelength spread, give excellent agreement between theory and experiment.

Consequently we also show in Fig. 2 calculations with the Darwin width increased to $5{\cdot}7\times10^{-3}$ °. There is then very satisfactory agreement between the calculations and experiment.

There are two possible reasons why the agreement is better with a larger-than-theoretical Darwin width. It may be that the germanium is not perfect, but has a small mosaic width in addition to the Darwin width. Alternatively, it may be that the Gaussian approximation underestimates the width because the Darwin curve is not of a Gaussian form. The convolution of two equal-width Gaussians gives a Gaussian of width $\sqrt{2}$ larger than a single Gaussian, whereas the convolution of two Lorentzians gives a curve of twice the width. The larger width may then result from the inadequacy of the Gaussian approximation to the Darwin curve. Evidence against this latter suggestion is provided by the numerical convolution theory described in the next section. The widths calculated with this theory are also too small, suggesting that the reason for the discrepancy is that the germanium monochromator and analyser crystals are not perfect.

The results of the experiments performed with poor-quality germanium monochromator and analyser and a GaAs sample are shown in Fig. 3. In this case corrections for the Darwin width of GaAs are negligible. The widths were calculated by adjusting the mosaic widths of the monochromator and analyser, and a good description of the transverse widths was obtained when these both had a width of 0·023°, as shown in Fig. 3. The measured mosaic spread of the monochromator crystal was 0·021°. The longitudinal widths are then in good agreement with experiment for wave vectors greater than 4 Å^{-1}, but at smaller wave vectors the observed widths are significantly smaller than those calculated. We do not understand the origin of this discrepancy.

In Fig. 4 we show the results obtained with the pyrolytic-graphite monochromator and analyser together with the InP sample. The mosaic spread of the graphite crystals was found by adjusting the calculated transverse widths to give agreement with experiment when $\eta_M = 0{\cdot}29°$. Calculations of the longitudinal width were then made with a wavelength spread equal to the width of the $K\alpha_1$ line, shown by the dotted line, and with $\Delta\lambda/\lambda = 2{\cdot}5\times10^{-3}$, the separation between the $K\alpha_1$ and $K\alpha_2$ lines. These calculations clearly give a good description of the experimental results.

2. *The convolution theory*

The reflectivity of perfect crystals is described by the Darwin curve rather than a Gaussian curve and therefore a detailed description of the resolution function of a triple-crystal X-ray diffractometer requires a convolution of Darwin profiles. This was first performed by Pynn *et al.* (1983) but they considered only the central part of the resolution function. The calculations have now been extended by Gartstein (1989) to obtain a more detailed form of the intensity distribution around Bragg reflections. We shall not repeat the details of the calculations here but merely comment that accurate numerical calculations require a careful treatment of the different rays in the diffractometer, leading to quite lengthy numerical convolutions.

Calculations were performed to compare with the observed scattering for three reflections, 400, 420 and 44$\bar{0}$, taking into account the Darwin widths of the InP sample. The results are shown as contour maps in Figs. 5–7, with the same contour levels as those plotted for the experiment. Clearly there is reasonable agreement between experiment and theory, although the experimental results are slightly broader in the direction perpendicular to the wave-vector transfer.

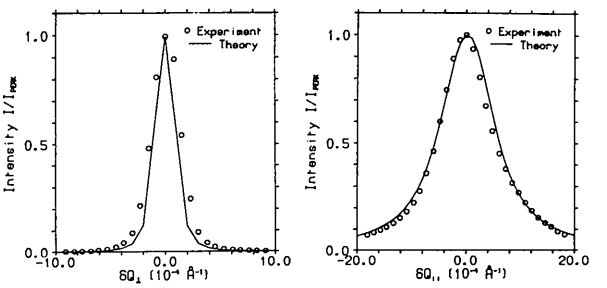

Fig. 9. The longitudinal and transverse profiles through the InP 400 reflection as measured and as calculated with the convolution theory using the nominal Darwin-width values for the high-resolution configuration.

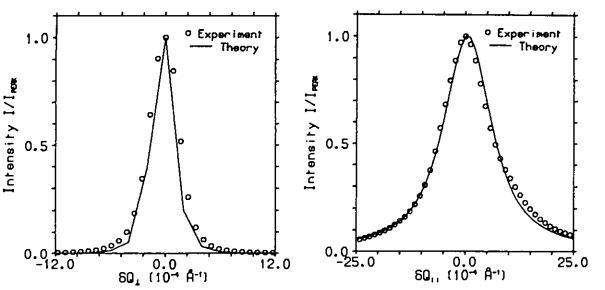

Fig. 10. The InP 420 reflection as for Fig. 9.

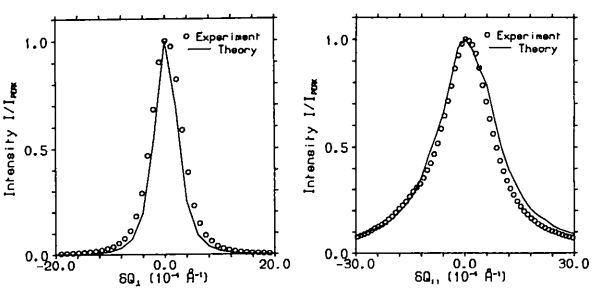

Fig. 11. The InP 44$\bar{0}$ reflection as for Fig. 9.

An alternative comparison is of the longitudinal and transverse scans through the centres of the Bragg reflections, and these are shown in Figs. 9–11. The theoretical transverse widths are systematically smaller than the measured widths by about 20%, in reasonable agreement with the discrepancy between the Gaussian theory and the measured transverse widths shown in Fig. 2. The longitudinal widths for the 400 and 420 reflections are in good agreement with experiment but the calculation for the $4\bar{4}0$ reflection is slightly broader than expected. This may be due to a reduction in the wavelength spread caused by the positioning of the pre-monochromator slit in the experiment.

IV. Concluding remarks

In this paper we have presented a detailed theoretical and experimental study of the resolution function of a triple-crystal X-ray diffractometer based on a rotating-anode source. Two different theories are compared with the experimental results.

In the Gaussian approximation theory, analytic and relatively simple expressions are used to calculate the widths of the central part of the resolution function. The comparison with experiment shows that the theory predicts the widths with an accuracy of better than 25% for a variety of different diffractometer configurations. The accuracy is improved if the Darwin widths of the monochromator and analyser crystals are adjusted to fit the data at one wave-vector transfer.

A more complicated theory, involving numerical convolution of the Darwin profiles, enables the detailed form of the resolution function to be calculated in the high-resolution configuration. This theory not only successfully describes the central part of the resolution function, but also the qualitative features of the scattered intensity away from the Bragg peak. The streaks, which appear at low intensity levels, are caused by the asymmetric form of the monochromator and analyser response functions. A simple account of the origin and direction of the streaks is given in § II.2. Unfortunately a detailed description requires a full knowledge of the monochromator and analyser response functions. These depend critically on the surface roughness of the crystals which is not usually controlled in an experiment.

We are grateful for the technical support of H. Vass, and for the financial support of the Science and Engineering Research Council.

References

ANDREWS, S. R. & COWLEY, R. A. (1985). *J. Phys. C*, **18**, 6427–6439.
ANDREWS, S. R. & COWLEY, R. A. (1986). *J. Phys. C*, **19**, 615–635.
BATTERMAN, B. & COLE, H. (1964). *Rev. Mod. Phys.* **36**, 681–717.
BJERRUM-MØLLER, H. & NIELSEN, M. (1970). *Instrumentation for Neutron Inelastic Scattering Research*, pp. 49–76. Vienna: International Atomic Energy Agency.
CHESSER, N. J. & AXE, J. D. (1973). *Acta Cryst.* A**29**, 160–169.
COOPER, M. J. & NATHANS, R. (1967). *Acta Cryst.* **23**, 357–367.
COWLEY, R. A. (1987). *Acta Cryst.* A**43**, 825–836.
COWLEY, R. A. & RYAN, T. W. (1987). *J. Phys. D*, **20**, 61–68.
GARTSTEIN, E. (1989). In preparation.
PYNN, R., FUJII, Y. & SHIRANE, G. (1983). *Acta Cryst.* A**39**, 38–46.
ROBINSON, I. K. (1986). *Phys. Rev. B*, **33**, 3830–3836.
RYAN, T. W. (1986). PhD thesis. Univ. of Edinburgh, Scotland.
RYAN, T. W., NELMES, R. J., COWLEY, R. A. & GIBAUD, A. (1986). *Phys. Rev. Lett.* **56**, 2704–2707.
STEDMAN, R. (1968). *Rev. Sci. Instrum.* **39**, 878–883.
ZACHARIASEN, W. H. (1945). *Theory of X-ray Diffraction in Crystals*. New York: Wiley.

Acta Cryst. (1989). A**45**, 422–427

Distortion of the Zeroth-Order Laue-Zone Pattern Caused by Dislocations in a Silicon Crystal*

BY JIANGUO WEN, RENHUI WANG AND GANGHUA LU†

Department of Physics, Wuhan University, 430072 *Wuhan, People's Republic of China*

(*Received* 7 *November* 1988; *accepted* 18 *January* 1989)

Abstract

The effect of dislocations in a silicon single crystal on the zeroth-order Laue-zone (ZOLZ) pattern in large-angle convergent-beam electron diffraction (LACBED) has been studied experimentally. It is found that edge dislocations cause the ZOLZ pattern to be compressed or elongated and screw dislocations cause it to be dislocated. This phenomenon is the consequence of opposite shifts of the two halves of the Tanaka pattern, separated by the shadow image of the dislocation line along directions **b** and $-\mathbf{b}$ of the Burgers vector. The shift direction of each half

* Project supported by the National Natural Science Foundation of China.

† Also with Laboratory of Atomic Image of Solids, Institute of Metal Research, Academia Sinica, 110015 Shenyang, People's Republic of China.

0108-7673/89/060422-06$03.00